


Observation of Significant Flavor-SU(3) Breaking in the Kaon Wave Function at $12 < Q^2 < 25 \text{ GeV}^2$ and Discovery of the Charmless Decay $\psi(3770) \rightarrow K_S^0 K_L^0$

M. Ablikim *et al.**
(BESIII Collaboration)

 (Received 19 December 2023; revised 11 February 2024; accepted 13 February 2024; published 25 March 2024)

We present cross sections for the reaction $e^+e^- \rightarrow K_S^0 K_L^0$ at center-of-mass energies ranging from 3.51 to 4.95 GeV using data samples collected in the BESIII experiment, corresponding to a total integrated luminosity of 26.5 fb^{-1} . The ratio of neutral-to-charged kaon form factors at large momentum transfers ($12 < Q^2 < 25 \text{ GeV}^2$) is determined to be 0.21 ± 0.01 , which indicates a small but significant effect of flavor-SU(3) breaking in the kaon wave function, and, consequently, excludes the possibility that flavor-SU(3) breaking is the primary reason for the strong experimental violation of the pQCD prediction $|F(\pi^\pm)|/|F(K^\pm)| = f_\pi^2/f_K^2$, where $F(\pi^\pm)$ and $F(K^\pm)$ are the form factors, and f_π and f_K are the decay constants of charged pions and kaons, respectively. We also observe a significant signal for the charmless decay $\psi(3770) \rightarrow K_S^0 K_L^0$ for the first time. Within a 1σ contour of the likelihood value, the branching fraction for $\psi(3770) \rightarrow K_S^0 K_L^0$ is determined to be $\mathcal{B} = (2.63^{+1.40}_{-1.59}) \times 10^{-5}$, and the relative phase between the continuum and $\psi(3770)$ amplitudes is $\phi = (-0.39^{+0.05}_{-0.10})\pi$. The branching fraction is in good agreement with the \mathcal{S} - and \mathcal{D} -wave charmonia mixing scheme proposed in the interpretation of the “ $\rho\pi$ puzzle” between J/ψ and $\psi(3686)$ decays.

DOI: [10.1103/PhysRevLett.132.131901](https://doi.org/10.1103/PhysRevLett.132.131901)

Understanding the internal quark-gluon structure of hadrons based on quantum chromodynamics (QCD) has been one of the fundamental aims of nuclear and particle physics. An important tool to achieve such a goal is to measure the electromagnetic form factors of hadrons at large momentum transfers (Q^2), where a photon acts as a probe that allows us to see the electric charges of the quarks and gluons inside of the hadron, rather than just the composite hadron [1,2]. Kaons are of great interest because their constituent quarks differ in mass by more than 1 order of magnitude, which leads to a broken flavor-SU(3) symmetry in the wave function and thus the form factor of neutral kaons develops an asymmetric component and deviates from zero [3]. The measurements of the electromagnetic form factors of kaons at large momentum transfers provide a sensitive measure of flavor-SU(3) breaking effects, estimated by the ratio of the form factors $|F_{K_S^0 K_L^0}(Q^2)|/|F_{K^+ K^-}(Q^2)|$. A value close to 1 indicates that the flavor-SU(3) breaking has a significant influence on the kaon’s wave function, while a value close to 0 indicates a minor effect [3]. Furthermore, this measurement

also provides valuable insights into the hypothesis [3] that flavor-SU(3) breaking may be the primary factor responsible for the large deviation between the perturbative QCD (pQCD) prediction $|F(\pi^\pm)|/|F(K^\pm)| = f_\pi^2/f_K^2$ [4,5] and the experimental results $|F(\pi^\pm)|/|F(K^\pm)| = 1.09 \pm 0.04$ at $|Q^2| = 17.4 \text{ GeV}^2$ [6] and $f_\pi^2/f_K^2 = 0.84 \pm 0.01$ [7]. Here $F(\pi^\pm)$ and $F(K^\pm)$ are the form factors, and f_π and f_K are the decay constants of charged pions and kaons, respectively.

The $K_S^0 K_L^0$ final state of vector charmonium decays is particularly interesting to understand the violation of the “12% rule” [8–11], where $\mathcal{Q}_h = \{\mathcal{B}[\psi(3686) \rightarrow h]/\mathcal{B}(J/\psi \rightarrow h)\} = (13.3 \pm 0.3)\%$ according to pQCD [7]. However, $\mathcal{Q}_{K_S^0 K_L^0}$ is found to be $(27.2 \pm 3.6)\%$ which deviates from the 12% rule by more than 3σ [12,13]. Here we focus on an explanation proposed by Rosner using \mathcal{S} - and \mathcal{D} -wave charmonia mixing [14], where the $\psi(3686)$ and $\psi(3770)$ are considered to be mixtures of the $\psi(2^3S_1)$ and $\psi(1^3D_1)$ states. In this scenario, the branching fraction of $\psi(3770) \rightarrow K_S^0 K_L^0$ is predicted to be within $[0.07 \pm 0.05, 3.7 \pm 1.6] \times 10^{-5}$ [15].

Theoretical studies on the form factors at large momentum transfers based on different models have so far yielded conflicting results on the flavor-SU(3) breaking effects of kaons [16–20], while experimental measurements are limited to small momentum transfers ($|Q^2| < 9.49 \text{ GeV}^2$) [21,22]. No significant signal was observed at the $\psi(3770)$ peak before [23,24], and only 4 events are observed with an

*Full author list given at the end of the Letter.

Published by the American Physical Society under the terms of the [Creative Commons Attribution 4.0 International license](https://creativecommons.org/licenses/by/4.0/). Further distribution of this work must maintain attribution to the author(s) and the published article’s title, journal citation, and DOI. Funded by SCOAP³.

expectation of 0.3 background events at $\sqrt{s} = 4.17$ GeV in the CLEO-c data [25], corresponding to a statistical significance of 3.6σ .

In this Letter, we report the electromagnetic form factors of neutral kaons measured with 26.5 fb^{-1} of data taken at center-of-mass (c.m.) energies (\sqrt{s}) from 3.51 to 4.95 GeV (i.e., $12 < Q^2 < 25 \text{ GeV}^2$) [26–30]. We also report the first observation of the charmless decay $\psi(3770) \rightarrow K_S^0 K_L^0$ and discuss its impact on our understanding of charmonium decay dynamics. The data was recorded with the BESIII detector, which is described in detail in Ref. [31]. Simulated data samples produced with a GEANT4-based [32] Monte Carlo (MC) package, which includes the geometric description of the BESIII detector and the detector response, are used to determine detection efficiencies and to estimate backgrounds. The simulation models the beam energy spread and initial state radiation (ISR) in the e^+e^- annihilations with the generator KKMC [33,34]. Signal Monte Carlo samples of $e^+e^- \rightarrow K_S^0 K_L^0$ are generated at each energy point with the vector-scalar-scalar (vss) model in which a vector particle decays into two scalars in EVTGEN [35,36], and the subsequent decay $K_S^0 \rightarrow \pi^+\pi^-$ is generated uniformly in phase space. To estimate the possible background, two kinds of exclusive MC samples are generated, which are $e^+e^- \rightarrow \gamma^{\text{ISR}}\psi(3686)$ with $\psi(3686) \rightarrow K_S^0 K_L^0$, and $e^+e^- \rightarrow K^{*0}(892)\bar{K}^0 + \text{c.c.}$ with $K^{*0}(892) \rightarrow \pi^0 K_{S/L}^0$, $\pi^0 \rightarrow \gamma\gamma$ and $\bar{K}^0 \rightarrow K_{L/S}^0$. The inclusive MC samples generated at $\sqrt{s} = 3.774$ GeV are used to study potential background. These samples include the production of $D\bar{D}$ pairs, the non- $D\bar{D}$ decays of the $\psi(3770)$, the ISR production of the J/ψ and $\psi(3686)$ states, and the continuum processes incorporated in KKMC.

Signal events contain a single K_S^0 reconstructed with $K_S^0 \rightarrow \pi^+\pi^-$. The K_L^0 is identified from the momentum difference between the K_S^0 and e^+e^- , assuming momentum conservation. We retain signal events which have two charged tracks and either have no neutral clusters, in the case that the K_L^0 passes through the detector without interaction, or has special neutral clusters found in the expected K_L^0 direction, in the case that the K_L^0 interacts with the detector material. Neutral clusters reconstructed in the detector but not in the expected K_L^0 direction are used to suppress background.

For each good charged track detected in the multilayer drift chamber (MDC), the polar angle (θ) is required to be within a range of $|\cos\theta| < 0.93$, where θ is defined with respect to the z axis, which is the symmetric axis of the MDC. Exactly two good charged tracks with zero net charge are required. The deposited energy of each track in the electromagnetic calorimeter (EMC) is required to be less than 1.2 GeV to suppress Bhabha events. Particle identification is applied where the specific ionization energy loss dE/dx measured by the MDC and the flight

time measured by the time-of-flight (TOF) detector form likelihoods $\mathcal{L}(h)(h = e, \pi)$ for each particle hypothesis. Both tracks are required to be identified as pions with $\mathcal{L}(\pi) > 0.001$ and $\mathcal{L}(\pi) > \mathcal{L}(e)$.

If two charged tracks fulfill these criteria they are assigned as a $\pi^+\pi^-$ pair. They are constrained to originate from a secondary vertex of a K_S^0 decay. The decay length of the K_S^0 candidates starting from the interaction point (IP) is required to be greater than 2 cm and greater than twice the vertex resolution to suppress $\gamma_{\text{ISR}}\mu\mu$ and $\gamma_{\text{ISR}}\rho^0(\rho^0 \rightarrow \pi^+\pi^-)$. The χ^2 of the secondary vertex fit is required to be less than 15, which is optimized using the figure of merit $\text{FOM} = (S/\sqrt{S+B})$. Here, S is the normalized number of events from the signal MC sample and B is the normalized number of background events estimated from the inclusive MC sample, which only contains the background without K_S^0 . The invariant mass of the K_S^0 candidate is required to be within $0.478 \text{ GeV}/c^2 < m_{\pi^+\pi^-} < 0.518 \text{ GeV}/c^2$. To further improve the resolution, a one-constraint (1C) kinematic fit is performed on the K_S^0 mass, and $\chi^2_{1\text{C}} < 12$ is further required.

Neutral clusters are identified using showers in the EMC. The deposited energy of each shower must be more than 25 MeV in the barrel region ($|\cos\theta| < 0.80$) and more than 50 MeV in the end cap region ($0.86 < |\cos\theta| < 0.92$). To suppress showers that originate from charged tracks, the angle subtended by the EMC shower and the position of the closest charged track at the EMC must be greater than 20° as measured from the IP. To suppress electronic noise and showers unrelated to the event, the difference between the EMC time and the event start time is required to be within $[0, 700]$ ns.

Pure $e^+e^- \rightarrow K_S^0 K_L^0$ ($K_S^0 \rightarrow \pi^+\pi^-$) events do not contain photons, so we keep events without neutral clusters in a K_L^0 cone defined as an area with an opening angle of 20° relative to the opposite direction of the K_S^0 in the e^+e^- c.m. frame. However, K_L^0 mesons may interact with the detector material and produce neutral clusters in the EMC. In this case, we examine K_L^0 candidates within the K_L^0 cone and require at least one neutral cluster satisfying a second moment [37] $[\Sigma_i(E_i r_i^2)/\Sigma_i(E_i)]$ greater than 20 cm^2 , where E_i is the deposited energy in the i th crystal and r_i refers to the radial distance of it from the cluster center. This requirement is useful to suppress $\gamma_{\text{ISR}}\mu\mu$ background since the neutral clusters produced by K_L^0 are wider than those produced by photons.

To suppress EMC noise and background events from $e^+e^- \rightarrow K^{*0}(892)\bar{K}^0 + \text{c.c.}$, where $K^{*0}(892)\bar{K}^0 \rightarrow \pi^0 K_S^0 K_L^0$, we require the total energy of the neutral clusters outside the cone to be less than 0.2 GeV. The invariant mass of every combination of two neutral clusters is calculated to search for π^0 candidates. Events where the invariant mass of any combination satisfies $M_{\gamma\gamma} \in [0.123, 0.144] \text{ GeV}/c^2$ are rejected.

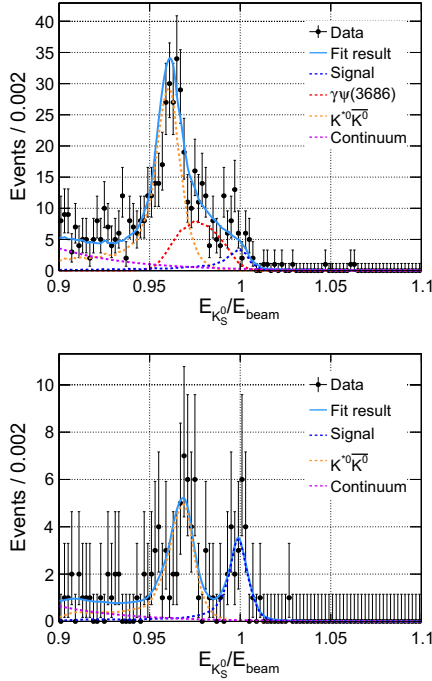


FIG. 1. Distributions of $X \equiv E_{K_S^0}/E_{\text{beam}}$ at $\sqrt{s} = 3.774$ (top) and 4.226 GeV (bottom), where the corresponding $\chi^2/\text{n.d.f.}$ of the fits are 1.06 and 0.50 , respectively. Dots with error bars are data. The blue solid lines are the total fit results, the blue dashed lines are the signal component, the red dashed lines represent the $e^+e^- \rightarrow \gamma^{\text{ISR}}\psi(3686)$ component, the orange dashed lines represent the $e^+e^- \rightarrow K^{*0}(892)\bar{K}^0 + \text{c.c.}$ component, and the violet dashed lines represent exponential functions describing the remaining background.

Figure 1 shows the $X \equiv E_{K_S^0}/E_{\text{beam}}$ distributions at $\sqrt{s} = 3.774$ and 4.226 GeV, where $E_{K_S^0}$ is the energy of the K_S^0 in the e^+e^- c.m. frame, and $E_{\text{beam}} = \sqrt{s}/2$ is the beam energy. Clear $e^+e^- \rightarrow K_S^0 K_L^0$ signals are observed at $X = 1$. The signal region defined as $X \in [0.98, 1.02]$ is used for the optimization of the selection criteria. Similar distributions are observed at the other c.m. energies.

An unbinned maximum likelihood fit is performed using the X distributions to extract the number of signal events. The definition of the likelihood can be found in the Supplemental Material [38]. Three simulated shapes derived from MC samples are used to describe the dominant components of the data: the signal component, the $e^+e^- \rightarrow \gamma^{\text{ISR}}\psi(3686)$ background, and the $e^+e^- \rightarrow K^{*0}(892)\bar{K}^0 + \text{c.c.}$ background. Each is convolved with a Gaussian function to account for the discrepancies in X (ΔX) and resolution ($\Delta\sigma$) between data and MC simulation. The $\Delta X = (3.8 \pm 0.8) \times 10^{-4}$ and $\Delta\sigma = (7.5 \pm 3.2) \times 10^{-4}$ are measured with the process $\psi(3686) \rightarrow K_S^0 K_L^0$, which increases the goodness-of-fit of data. The remaining background is described by an exponential function. The expected number of background events from the processes $e^+e^- \rightarrow \gamma^{\text{ISR}}\psi(3686)$ and $e^+e^- \rightarrow K^{*0}(892)\bar{K}^0 + \text{c.c.}$ in

the $\sqrt{s} = 3.774$ GeV data sample are calculated to be 147 ± 15 and 390 ± 22 using the corresponding integrated luminosity and cross sections [41]. They are fixed at their central values in the fit at $\sqrt{s} = 3.774$ GeV while floating at other energy points, the uncertainties are considered as one source of systematic uncertainty. The simulated shape of $e^+e^- \rightarrow \gamma^{\text{ISR}}\psi(3686)$ is only used at 3.710 and 3.774 GeV, its inclusion has negligible effects on the signal yield at other energy points. The parameters of the exponential function are determined from the fit at energy points with high luminosity. For energy points with low luminosity, the parameters extracted at the nearest high luminosity point are used.

The dressed cross section is determined as

$$\sigma^{\text{dressed}} = \frac{N^{\text{obs}}}{\varepsilon \cdot \mathcal{L} \cdot (1 + \delta) \cdot \mathcal{B}(K_S^0 \rightarrow \pi^+ \pi^-)}, \quad (1)$$

where N^{obs} is the number of signal events from the fit, \mathcal{L} is the integrated luminosity, and $\mathcal{B}(K_S^0 \rightarrow \pi^+ \pi^-) = (69.20 \pm 0.05)\%$ [7] is the branching fraction of $K_S^0 \rightarrow \pi^+ \pi^-$. The efficiency ε and the ISR correction factor $(1 + \delta)$ [42] are obtained iteratively following the procedure used in Ref. [39]. Figure 2(a) shows the resulting cross sections. We find that the cross sections are at a subpicobarn level and decrease gradually with increasing c.m. energy. The cross section at $\sqrt{s} = 3.774$ GeV, however, is significantly lower than the expected trend by more than 5σ , suggesting interference between the $e^+e^- \rightarrow K_S^0 K_L^0$ and $\psi(3770) \rightarrow K_S^0 K_L^0$ amplitudes.

We use the cross sections [excluding $\sqrt{s} = 3.774$ GeV data to avoid the $\psi(3770)$ resonance contribution] to calculate the electromagnetic form factors of the neutral kaon via

$$|F_{K_S^0 K_L^0}(s)|^2 = \frac{\sigma^{\text{dressed}} \cdot |1 - \Pi|^2 \cdot 3s}{\pi\alpha^2\beta^3}, \quad (2)$$

where α is the fine-structure constant, $\beta = \sqrt{1 - 4m_{K^0}^2/s}$ is the velocity of the K_S^0 in the laboratory system, and $(1/|1 - \Pi|^2)$ is the vacuum polarization factor [43]. Figure 2(b) shows the ratio of the neutral and the charged kaon form factors, where the data on charged kaons comes from Ref. [40]. We fit the ratios with polynomials of different orders and find the shape is close to constant at $|F_{K_S^0 K_L^0}/F_{K^+ K^-}| = 0.21 \pm 0.01$. The coefficients of higher-order polynomial terms are not significant ($< 2\sigma$) under hypothesis testing. The electromagnetic form factors of the neutral kaon and the ratio of neutral-to-charged kaon form factors at each c.m. energy are listed in the Supplemental Material [38].

The contribution of the $\psi(3770) \rightarrow K_S^0 K_L^0$ amplitude is determined using a maximum likelihood fit of the dressed

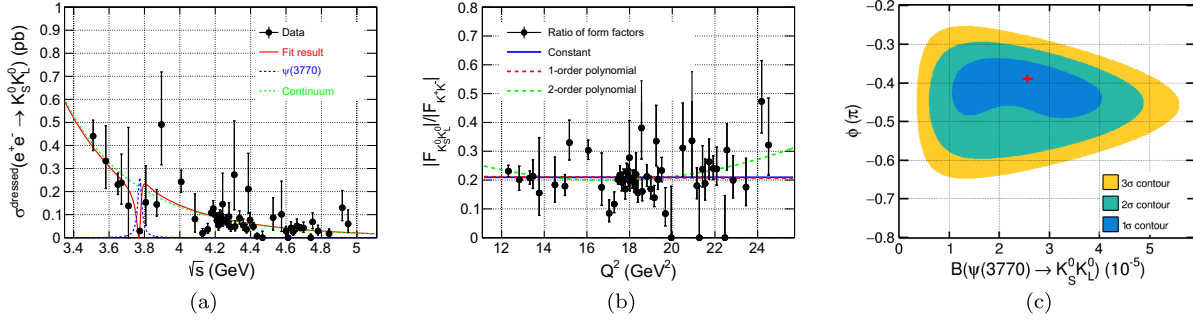


FIG. 2. (a) Dressed cross sections of $e^+e^- \rightarrow K_S^0 K_L^0$ and a fit with the coherent sum of a continuum and a $\psi(3770)$ resonance amplitude, using the local minimum in (c), where $B = 2.6 \times 10^{-5}$ and $\phi = -0.39\pi$. Dots with error bars are data. Red solid, green dashed, and blue dashed lines are the fit results, the continuum production, and the $\psi(3770)$ production, respectively. (b) The ratio of neutral-to-charged kaon form factors. The blue solid, red dashed, and green dashed lines result from fits with different order polynomials, the corresponding $\chi^2/\text{n.d.f}$ are 1.26, 1.28, 1.19, respectively. (c) The likelihood contours in the $B[\psi(3770) \rightarrow K_S^0 K_L^0]$ and the relative phase ϕ plane. The filled areas are up to 3σ likelihood contours. The red cross shows the local minimum.

cross section, which we describe as a coherent sum of a Breit-Wigner function for the $\psi(3770)$ amplitude and a power law function for the continuum amplitude:

$$\sigma^{\text{dressed}} = \left| BW \cdot e^{i\phi} + \frac{a}{(\sqrt{s})^n} \cdot \sqrt{\Phi(\sqrt{s})} \right|^2, \quad (3)$$

where $BW = [\sqrt{12\pi\Gamma_{ee}\Gamma\mathcal{B}}/(s - M^2 + iM\Gamma)] \sqrt{[\Phi(\sqrt{s})/\Phi(M)]}$ is the $\psi(3770)$ amplitude with M , Γ , Γ_{ee} , and \mathcal{B} being the mass, width, electronic width, and the branching fraction of $\psi(3770) \rightarrow K_S^0 K_L^0$, respectively; $\Phi(\sqrt{s}) = (q^3/s)$ is a \mathcal{P} -wave phase space factor, in which q is the $K_{S/L}^0$ momentum in the e^+e^- c.m. frame; ϕ is the relative phase between the continuum and $\psi(3770)$ amplitudes; The a and n are free parameters.

Without using the data at $\sqrt{s} = 3.774$ GeV, we fit the cross sections with the pure continuum amplitude and determine $a = (0.016 \pm 0.007) \text{ GeV}^{n-0.5} \text{ pb}^{0.5}$ and $n = 4.60 \pm 0.31$. By including the data at $\sqrt{s} = 3.774$ GeV and the $\psi(3770)$ resonance amplitude, with the mass, width, and electronic width of the $\psi(3770)$ fixed at their world average values [7], we perform a likelihood scan in the B versus ϕ plane. In this scan, the a and n are allowed to float until they reach the local minimum within their parameter space. The results are shown in Fig. 2(c). A clear region of local minima was observed through the scan, the B and ϕ are determined to be $(2.63_{-1.59}^{+1.40}) \times 10^{-5}$ and $(-0.39_{-0.10}^{+0.05})\pi$ within 1σ likelihood contour. Figure 2(a) shows the fit result corresponding to the local minimum. The significance of the $\psi(3770)$ resonance contribution is determined to be 10σ in comparison to an alternative fit without including the resonance. This indicates that the charmless decay $\psi(3770) \rightarrow K_S^0 K_L^0$ is observed for the first time. The tests for other 1^{--} resonances such as $\psi(4160)$ result in a significance less than 3σ .

The systematic uncertainties of the cross section measurement are listed in Table I, where the total systematic uncertainty is the square root of the quadratic sum of all sources, assuming they are independent. The uncertainty of the integrated luminosity is 1.0% [26–30]. The difference in the tracking efficiency between data and MC simulation is 1.0% per track [44]. The uncertainties of the K_S^0 reconstruction, the K_L^0 requirements, and the π^0 rejection are estimated with control samples and the efficiency differences between data and MC simulation are measured following the method in Ref. [45]. We use $\psi(3770) \rightarrow K^{*0}(892)\bar{K}^0$, with $K^{*0}(892) \rightarrow K^\pm\pi^\mp$ and $\bar{K}^0 \rightarrow K_S^0$ to determine an uncertainty of 1.3% for the K_S^0 reconstruction after multiplying by a correction factor of 1.018 to the MC efficiency. Using the control sample $\psi(3686) \rightarrow K_S^0 K_L^0$, we find that the K_L^0 acceptance rate in MC simulation is $(5.0 \pm 0.5)\%$ higher compared to data, therefore we correct the MC efficiency and quote an uncertainty of 0.5%. Similarly for the π^0 rejection, the rate in MC simulation is $(3.0 \pm 0.4)\%$ lower compared to data, therefore we correct the MC efficiency and quote an uncertainty of 0.4%.

To study the uncertainties resulting from our choice of signal and background shapes when extracting the number of signal events, we select five data samples with large statistics to avoid statistical fluctuations, namely at c.m. energies of $\sqrt{s} = 3.510, 3.650, 3.774, 4.178,$ and 4.226 GeV. The uncertainty resulting from the fixed parameters of the Gaussian function is estimated by varying the parameter values within 1σ . The difference in the signal yields is negligible ($< 0.5\%$) except for 3.774 GeV, which are 1.2% for ΔX and 2.7% for $\Delta\sigma$. The numbers of $e^+e^- \rightarrow \gamma^{\text{ISR}}\psi(3686)$ and $e^+e^- \rightarrow K^{*0}(892)\bar{K}^0 + \text{c.c.}$ events are fixed in the fit at $\sqrt{s} = 3.774$ GeV, and differences are estimated by varying them by 1σ around their central values. The resulting uncertainty is 7.8% for $e^+e^- \rightarrow \gamma^{\text{ISR}}\psi(3686)$ and 0.9% for $e^+e^- \rightarrow K^{*0}(892)\bar{K}^0 + \text{c.c.}$, respectively. We perform alternative fits by replacing the

TABLE I. Relative systematic uncertainties of the cross section measurements.

Source	Systematic uncertainty (%)
Luminosity	1.0
Tracking	2.0
K_S^0 reconstruction	1.3
K_L^0 requirements	0.5
π^0 rejection	0.4
Fitting line shape	4.7
Total	5.4

exponential function with the background shape extracted from the inclusive MC sample. The relative differences in the signal yields are 2.6%, 2.8%, 4.3%, 1.9%, and 1.8% for the selected data samples. Therefore, after combining the uncertainties at 3.774 GeV, a luminosity-weighted uncertainty of 4.7% is taken as the systematic uncertainty caused by the line shapes used in the fits for all energy points. The uncertainty from the fitting range is examined by the ‘‘Barlow test’’ [46]. We choose 20 different fixed-length fitting ranges with a step size of 1 MeV to compare the deviation between different measurements. We find these deviations are due to statistical fluctuations and are thereby ignored in the systematic uncertainty. The uncertainty from the branching fraction of $K_S^0 \rightarrow \pi^+\pi^-$ is less than 0.1% according to the Particle Data Group, which is ignored.

In summary, we measure the electromagnetic form factors of the neutral kaons at large momentum transfers from 12 to 25 GeV² for the first time, which are consistent with previous measurement at 17.4 GeV² [25]. The constant ratio (0.21 ± 0.01) of neutral-to-charged kaon form factors we obtained indicates a small but significant effect of flavor-SU(3) breaking on the kaon wave function, and consequently excludes the possibility that flavor-SU(3) breaking is the primary reason for the large observed deviation between the pQCD prediction and the experimental result. The observed constant ratio of the kaon form factors is also in disagreement with the predicted trend using a single bound-state interaction kernel [16], providing more information for the investigation of the internal structure of neutral kaons.

We observe a significant signal of $\psi(3770) \rightarrow K_S^0 K_L^0$ for the first time. This is the first discovery of the charmless decay of the $\psi(3770)$ with a statistical significance exceeding 5σ . Within the 1σ contour of the likelihood value, the branching fraction of $\psi(3770) \rightarrow K_S^0 K_L^0$ is determined to be $\mathcal{B} = (2.63_{-1.59}^{+1.40}) \times 10^{-5}$, and the relative phase between the continuum amplitude and the $\psi(3770)$ decay amplitude is $\phi = (-0.39_{-0.10}^{+0.05})\pi$. The uncertainties are mainly due to insufficient data points near the $\psi(3770)$ peak, thus a finer scan around the $\psi(3770)$ will help to reveal the nature of the $\psi(3770)$. The branching fraction is in good agreement

with the prediction [15] of the \mathcal{S} - and \mathcal{D} -wave charmonia mixing model developed to interpret the ‘‘ $\rho\pi$ puzzle’’ between J/ψ and $\psi(3686)$ decays [14]. Assuming a negligible contribution [47] from the electromagnetic $\psi(3770)$ amplitude, a phase ϕ , around $-(\pi/2)$, supports the proposition [48] that the relative phase between strong and electromagnetic charmonium decay amplitudes is universally $-(\pi/2)$ and agrees with experimental measurements in various final states [49].

The BESIII Collaboration thanks the staff of BEPCII and the IHEP computing center for their strong support. This work is supported in part by National Key R&D Program of China under Contracts No. 2020YFA0406300, No. 2020YFA0406400; National Natural Science Foundation of China (NSFC) under Contracts No. 11635010, No. 11735014, No. 11835012, No. 11935015, No. 11935016, No. 11935018, No. 11961141012, No. 12025502, No. 12035009, No. 12035013, No. 12061131003, No. 12192260, No. 12192261, No. 12192262, No. 12192263, No. 12192264, No. 12192265, No. 12221005, No. 12225509, No. 12235017; the Chinese Academy of Sciences (CAS) Large-Scale Scientific Facility Program; the CAS Center for Excellence in Particle Physics (CCEPP); Joint Large-Scale Scientific Facility Funds of the NSFC and CAS under Contract No. U1832207; CAS Key Research Program of Frontier Sciences under Contracts Nos. QYZDJ-SSW-SLH003, QYZDJ-SSW-SLH040; 100 Talents Program of CAS; The Institute of Nuclear and Particle Physics (INPAC) and Shanghai Key Laboratory for Particle Physics and Cosmology; European Union’s Horizon 2020 research and innovation programme under Marie Skłodowska-Curie grant agreement under Contract No. 894790; German Research Foundation DFG under Contracts No. 455635585, Collaborative Research Center CRC 1044, FOR5327, GRK 2149; Istituto Nazionale di Fisica Nucleare, Italy; Ministry of Development of Turkey under Contract No. DPT2006K-120470; National Research Foundation of Korea under Contract No. NRF-2022R1A2C1092335; National Science and Technology fund of Mongolia; National Science Research and Innovation Fund (NSRF) via the Program Management Unit for Human Resources & Institutional Development, Research and Innovation of Thailand under Contract No. B16F640076; Polish National Science Centre under Contract No. 2019/35/O/ST2/02907; The Swedish Research Council; U.S. Department of Energy under Contract No. DE-FG02-05ER41374.

- [1] G. A. Miller, M. Strikman, and C. Weiss, *Phys. Rev. D* **83**, 013006 (2011).
 [2] E. B. Dally, D. J. Drickey, J. M. Hauptman, C. F. May, and D. H. Stork, *Phys. Rev. D* **24**, 1718 (1981).

- [3] G. P. Lepage and S. J. Brodsky, *Phys. Rev. D* **22**, 2157 (1980).
- [4] G. R. Farrar and D. R. Jackson, *Phys. Rev. Lett.* **43**, 246 (1979).
- [5] G. P. Lepage and S. J. Brodsky, *Phys. Lett.* **87B**, 359 (1979).
- [6] K. K. Seth, S. Dobbs, Z. Metreveli, A. Tomaradze, T. Xiao, and G. Bonvicini, *Phys. Rev. Lett.* **110**, 022002 (2013).
- [7] R. L. Workman *et al.* (Particle Data Group), *Prog. Theor. Exp. Phys.* **2022**, 083C01 (2022).
- [8] M. E. B. Franklin *et al.*, *Phys. Rev. Lett.* **51**, 963 (1983).
- [9] J. Z. Bai *et al.* (BESIII Collaboration), *Phys. Rev. D* **69**, 072001 (2004).
- [10] J. Z. Bai *et al.* (BESIII Collaboration), *Phys. Rev. Lett.* **92**, 052001 (2004).
- [11] M. Ablikim *et al.* (BESIII Collaboration), *Phys. Lett. B* **614**, 37 (2005).
- [12] M. Ablikim *et al.* (BESIII Collaboration), *Phys. Rev. D* **96**, 112001 (2017).
- [13] J. Z. Bai *et al.* (BESIII Collaboration), *Phys. Rev. Lett.* **92**, 052001 (2004).
- [14] J. L. Rosner, *Phys. Rev. D* **64**, 094002 (2001).
- [15] P. Wang, X. H. Mo, and C. Z. Yuan, *Phys. Rev. D* **70**, 077505 (2004).
- [16] F. Gao, L. Chang, Y. X. Liu, C. D. Roberts, and P. C. Tandy, *Phys. Rev. D* **96**, 034024 (2017).
- [17] V. L. Chernyak, A. R. Zhitnitsky, and I. R. Zhitnitsky, *Nucl. Phys.* **B204**, 477 (1982).
- [18] V. L. Chernyak and A. R. Zhitnitsky, *Phys. Rep.* **112**, 173 (1984).
- [19] V. M. Braun *et al.*, *Phys. Rev. D* **74**, 074501 (2006).
- [20] S. J. Brodsky and G. F. de Teramond, *Subnuclear Ser.* **45**, 139 (2009).
- [21] F. Mane, D. Bisello, J. C. Bizot, J. Buon, A. Cordier, and B. Delcourt, *Phys. Lett.* **99B**, 261 (1981).
- [22] M. Ablikim *et al.* (BESIII Collaboration), *Phys. Rev. D* **104**, 092014 (2021).
- [23] M. Ablikim *et al.* (BESIII Collaboration), *Phys. Rev. D* **70**, 077101 (2004).
- [24] D. Cronin-Hennessy *et al.* (CLEO Collaboration), *Phys. Rev. D* **74**, 012005 (2006).
- [25] K. K. Seth, S. Dobbs, A. Tomaradze, T. Xiao, and G. Bonvicini, *Phys. Lett. B* **730**, 332 (2014).
- [26] M. Ablikim (BESIII Collaboration), *Chin. Phys. C* **37**, 123001 (2013).
- [27] M. Ablikim *et al.* (BESIII Collaboration), *Chin. Phys. C* **40**, 063001 (2016).
- [28] M. Ablikim *et al.* (BESIII Collaboration), *Chin. Phys. C* **45**, 103001 (2021).
- [29] M. Ablikim *et al.* (BESIII Collaboration), *Chin. Phys. C* **46**, 113002 (2022).
- [30] M. Ablikim *et al.* (BESIII Collaboration), *Chin. Phys. C* **46**, 113003 (2022).
- [31] M. Ablikim *et al.* (BESIII Collaboration), *Nucl. Instrum. Methods Phys. Res., Sect. A* **614**, 345 (2010).
- [32] S. Agostinelli *et al.* (GEANT4 Collaboration), *Nucl. Instrum. Methods Phys. Res., Sect. A* **506**, 250 (2003).
- [33] S. Jadach, B. F. L. Ward, and Z. Was, *Phys. Rev. D* **63**, 113009 (2001).
- [34] S. Jadach, B. F. L. Ward, and Z. Was, *Comput. Phys. Commun.* **130**, 260 (2000).
- [35] D. J. Lange, *Nucl. Instrum. Methods Phys. Res., Sect. A* **462**, 152 (2001).
- [36] R. G. Ping, *Chin. Phys. C* **32**, 599 (2008).
- [37] V. Prasad, C. Liu, X. Ji, W. Li, H. Liu, and X. Lou, *Springer Proc. Phys.* **174**, 577 (2016).
- [38] See Supplemental Material at <http://link.aps.org/supplemental/10.1103/PhysRevLett.132.131901> including Refs. [39,40], for a summary of c.m. energies, integrated luminosities, signal yields, event selection efficiencies, ISR correction factors, vacuum polarization factors, and Born cross section. A summary of the electromagnetic form factors of the neutral kaon and the ratio of neutral-to-charged kaon form factors at nonresonant energy points. The definition of likelihood in signal extraction. The fit results at different energy points.
- [39] W. Sun, T. Liu, M. Jing, L. Wang, B. Zhong, and W. Song, *Front. Phys.* **16**, 64501 (2021).
- [40] J. P. Lees *et al.* (BABAR Collaboration), *Phys. Rev. D* **92**, 072008 (2015).
- [41] G. S. Adams *et al.* (CLEO Collaboration), *Phys. Rev. D* **73**, 012002 (2006).
- [42] E. A. Kuraev and V. S. Fadin, *Sov. J. Nucl. Phys.* **41**, 466 (1985), <https://api.semanticscholar.org/CorpusID:124372625>.
- [43] S. Actis *et al.* (Working Group on Radiative Corrections and Monte Carlo Generators for Low Energies), *Eur. Phys. J. C* **66**, 585 (2010).
- [44] M. Ablikim *et al.* (BESIII Collaboration), *Phys. Rev. D* **99**, 031101 (2019).
- [45] M. Ablikim *et al.* (BESIII Collaboration), *Phys. Rev. D* **106**, 052012 (2022).
- [46] R. Barlow, [arXiv:hep-ex/0207026](https://arxiv.org/abs/hep-ex/0207026).
- [47] P. Wang, C. Z. Yuan, X. H. Mo, and D. H. Zhang, *Phys. Lett. B* **593**, 89 (2004).
- [48] P. Wang, *Frascati Phys. Ser.* **42**, 171 (2006).
- [49] K. Zhu, X. H. Mo, and C. Z. Yuan, *Int. J. Mod. Phys. A* **30**, 1550148 (2015).

M. Ablikim,¹ M. N. Achasov,^{4,b} P. Adlarson,⁷⁵ X. C. Ai,⁸¹ R. Aliberti,³⁵ A. Amoroso,^{74a,74c} M. R. An,³⁹ Q. An,^{71,58} Y. Bai,⁵⁷ O. Bakina,³⁶ I. Balossino,^{29a} Y. Ban,^{46,g} H.-R. Bao,⁶³ V. Batzskaya,^{1,44} K. Begzsuren,³² N. Berger,³⁵ M. Berlowski,⁴⁴ M. Bertani,^{28a} D. Bettoni,^{29a} F. Bianchi,^{74a,74c} E. Bianco,^{74a,74c} A. Bortone,^{74a,74c} I. Boyko,³⁶ R. A. Briere,⁵ A. Brueggemann,⁶⁸ H. Cai,⁷⁶ X. Cai,^{1,58} A. Calcaterra,^{28a} G. F. Cao,^{1,63} N. Cao,^{1,63} S. A. Cetin,^{62a} J. F. Chang,^{1,58} T. T. Chang,⁷⁷ W. L. Chang,^{1,63} G. R. Che,⁴³ G. Chelkov,^{36,a} C. Chen,⁴³ Chao Chen,⁵⁵ G. Chen,¹ H. S. Chen,^{1,63} M. L. Chen,^{1,58,63} S. J. Chen,⁴² S. L. Chen,⁴⁵ S. M. Chen,⁶¹ T. Chen,^{1,63} X. R. Chen,^{31,63} X. T. Chen,^{1,63} Y. B. Chen,^{1,58} Y. Q. Chen,³⁴ Z. J. Chen,^{25,h} S. K. Choi,¹⁰ X. Chu,⁴³ G. Cibinetto,^{29a} S. C. Coen,³ F. Cossio,^{74c} J. J. Cui,⁵⁰ H. L. Dai,^{1,58}

J. P. Dai,⁷⁹ A. Dbeysi,¹⁸ R. E. de Boer,³ D. Dedovich,³⁶ Z. Y. Deng,¹ A. Denig,³⁵ I. Denysenko,³⁶ M. Destefanis,^{74a,74c}
 F. De Mori,^{74a,74c} B. Ding,^{66,1} X. X. Ding,^{46,g} Y. Ding,⁴⁰ Y. Ding,³⁴ J. Dong,^{1,58} L. Y. Dong,^{1,63} M. Y. Dong,^{1,58,63} X. Dong,⁷⁶
 M. C. Du,¹ S. X. Du,⁸¹ Z. H. Duan,⁴² P. Egorov,^{36,a} Y. H. Fan,⁴⁵ J. Fang,^{1,58} S. S. Fang,^{1,63} W. X. Fang,¹ Y. Fang,¹
 Y. Q. Fang,^{1,58} R. Farinelli,^{29a} L. Fava,^{74b,74c} F. Feldbauer,³ G. Felici,^{28a} C. Q. Feng,^{71,58} J. H. Feng,⁵⁹ K. Fischer,⁶⁹
 M. Fritsch,³ C. D. Fu,¹ J. L. Fu,⁶³ Y. W. Fu,¹ H. Gao,⁶³ Y. N. Gao,^{46,g} Yang Gao,^{71,58} S. Garbolino,^{74c} I. Garzia,^{29a,29b}
 P. T. Ge,⁷⁶ Z. W. Ge,⁴² C. Geng,⁵⁹ E. M. Gersabeck,⁶⁷ A. Gilman,⁶⁹ K. Goetzen,¹³ L. Gong,⁴⁰ W. X. Gong,^{1,58} W. Gradl,³⁵
 S. Gramigna,^{29a,29b} M. Greco,^{74a,74c} M. H. Gu,^{1,58} Y. T. Gu,¹⁵ C. Y. Guan,^{1,63} Z. L. Guan,²² A. Q. Guo,^{31,63} L. B. Guo,⁴¹
 M. J. Guo,⁵⁰ R. P. Guo,⁴⁹ Y. P. Guo,^{12,f} A. Guskov,^{36,a} J. Gutierrez,²⁷ T. T. Han,¹ W. Y. Han,³⁹ X. Q. Hao,¹⁹ F. A. Harris,⁶⁵
 K. K. He,⁵⁵ K. L. He,^{1,63} F. H. H. Heinsius,³ C. H. Heinz,³⁵ Y. K. Heng,^{1,58,63} C. Herold,⁶⁰ T. Holtmann,³ P. C. Hong,^{12,f}
 G. Y. Hou,^{1,63} X. T. Hou,^{1,63} Y. R. Hou,⁶³ Z. L. Hou,¹ B. Y. Hu,⁵⁹ H. M. Hu,^{1,63} J. F. Hu,^{56,i} T. Hu,^{1,58,63} Y. Hu,¹
 G. S. Huang,^{71,58} K. X. Huang,⁵⁹ L. Q. Huang,^{31,63} X. T. Huang,⁵⁰ Y. P. Huang,¹ T. Hussain,⁷³ N. Hüsken,^{27,35}
 N. in der Wiesche,⁶⁸ M. Irshad,^{71,58} J. Jackson,²⁷ S. Jaeger,³ S. Janchiv,³² J. H. Jeong,¹⁰ Q. Ji,¹ Q. P. Ji,¹⁹ X. B. Ji,^{1,63}
 X. L. Ji,^{1,58} Y. Y. Ji,⁵⁰ X. Q. Jia,⁵⁰ Z. K. Jia,^{71,58} H. J. Jiang,⁷⁶ P. C. Jiang,^{46,g} S. S. Jiang,³⁹ T. J. Jiang,¹⁶ X. S. Jiang,^{1,58,63}
 Y. Jiang,⁶³ J. B. Jiao,⁵⁰ Z. Jiao,²³ S. Jin,⁴² Y. Jin,⁶⁶ M. Q. Jing,^{1,63} X. M. Jing,⁶³ T. Johansson,⁷⁵ X. Kui,¹ S. Kabana,³³
 N. Kalantar-Nayestanaki,⁶⁴ X. L. Kang,⁹ X. S. Kang,⁴⁰ M. Kavatsyuk,⁶⁴ B. C. Ke,⁸¹ V. Khachatryan,²⁷ A. Khoukaz,⁶⁸
 R. Kiuchi,¹ R. Kliemt,¹³ O. B. Kolcu,^{62a} B. Kopf,³ M. Kuessner,³ A. Kupsc,^{44,75} W. Kühn,³⁷ J. J. Lane,⁶⁷ P. Larin,¹⁸
 A. Lavania,²⁶ L. Lavezzi,^{74a,74c} T. T. Lei,^{71,58} Z. H. Lei,^{71,58} H. Leithoff,³⁵ M. Lellmann,³⁵ T. Lenz,³⁵ C. Li,⁴⁷ C. Li,⁴³
 C. H. Li,³⁹ Cheng Li,^{71,58} D. M. Li,⁸¹ F. Li,^{1,58} G. Li,¹ H. Li,^{71,58} H. B. Li,^{1,63} H. J. Li,¹⁹ H. N. Li,^{56,i} Hui Li,⁴³ J. R. Li,⁶¹
 J. S. Li,⁵⁹ J. W. Li,⁵⁰ Ke Li,¹ L. J. Li,^{1,63} L. K. Li,¹ Lei Li,⁴⁸ M. H. Li,⁴³ P. R. Li,^{38,k} Q. X. Li,⁵⁰ S. X. Li,¹² T. Li,⁵⁰ W. D. Li,^{1,63}
 W. G. Li,¹ X. H. Li,^{71,58} X. L. Li,⁵⁰ Xiaoyu Li,^{1,63} Y. G. Li,^{46,g} Z. J. Li,⁵⁹ Z. X. Li,¹⁵ C. Liang,⁴² H. Liang,^{1,63} H. Liang,^{71,58}
 Y. F. Liang,⁵⁴ Y. T. Liang,^{31,63} G. R. Liao,¹⁴ L. Z. Liao,⁵⁰ Y. P. Liao,^{1,63} J. Libby,²⁶ A. Limphirat,⁶⁰ D. X. Lin,^{31,63} T. Lin,¹
 B. J. Liu,¹ B. X. Liu,⁷⁶ C. Liu,³⁴ C. X. Liu,¹ F. H. Liu,⁵³ Fang Liu,¹ Feng Liu,⁶ G. M. Liu,^{56,i} H. Liu,^{38,j,k} H. B. Liu,¹⁵
 H. M. Liu,^{1,63} Huanhuan Liu,¹ Huihui Liu,²¹ J. B. Liu,^{71,58} J. Y. Liu,^{1,63} K. Liu,¹ K. Y. Liu,⁴⁰ Ke Liu,²² L. Liu,^{71,58} L. C. Liu,⁴³
 Lu Liu,⁴³ M. H. Liu,^{12,f} P. L. Liu,¹ Q. Liu,⁶³ S. B. Liu,^{71,58} T. Liu,^{12,f} W. K. Liu,⁴³ W. M. Liu,^{71,58} X. Liu,^{38,j,k} Y. Liu,^{38,j,k}
 Y. Liu,⁸¹ Y. B. Liu,⁴³ Z. A. Liu,^{1,58,63} Z. Q. Liu,⁵⁰ X. C. Lou,^{1,58,63} F. X. Lu,⁵⁹ H. J. Lu,²³ J. G. Lu,^{1,58} X. L. Lu,¹ Y. Lu,⁷
 Y. P. Lu,^{1,58} Z. H. Lu,^{1,63} C. L. Luo,⁴¹ M. X. Luo,⁸⁰ T. Luo,^{12,f} X. L. Luo,^{1,58} X. R. Lyu,⁶³ Y. F. Lyu,⁴³ F. C. Ma,⁴⁰ H. Ma,⁷⁹
 H. L. Ma,¹ J. L. Ma,^{1,63} L. L. Ma,⁵⁰ M. M. Ma,^{1,63} Q. M. Ma,¹ R. Q. Ma,^{1,63} X. Y. Ma,^{1,58} Y. Ma,^{46,g} Y. M. Ma,³¹ F. E. Maas,¹⁸
 M. Maggiora,^{74a,74c} S. Malde,⁶⁹ Q. A. Malik,⁷³ A. Mangoni,^{28b} Y. J. Mao,^{46,g} Z. P. Mao,¹ S. Marcello,^{74a,74c} Z. X. Meng,⁶⁶
 J. G. Messchendorp,^{13,64} G. Mezzadri,^{29a} H. Miao,^{1,63} T. J. Min,⁴² R. E. Mitchell,²⁷ X. H. Mo,^{1,58,63} B. Moses,²⁷
 N. Yu. Muchnoi,^{4,b} J. Muskalla,³⁵ Y. Nefedov,³⁶ F. Nerling,^{18,d} I. B. Nikolaev,^{4,b} Z. Ning,^{1,58} S. Nisar,^{11,1} Q. L. Niu,^{38,j,k}
 W. D. Niu,⁵⁵ Y. Niu,⁵⁰ S. L. Olsen,⁶³ Q. Ouyang,^{1,58,63} S. Pacetti,^{28b,28c} X. Pan,⁵⁵ Y. Pan,⁵⁷ A. Pathak,³⁴ P. Patteri,^{28a}
 Y. P. Pei,^{71,58} M. Pelizaes,³ H. P. Peng,^{71,58} Y. Y. Peng,^{38,j,k} K. Peters,^{13,d} J. L. Ping,⁴¹ R. G. Ping,^{1,63} S. Plura,³⁵ V. Prasad,³³
 F. Z. Qi,¹ H. Qi,^{71,58} H. R. Qi,⁶¹ M. Qi,⁴² T. Y. Qi,^{12,f} S. Qian,^{1,58} W. B. Qian,⁶³ C. F. Qiao,⁶³ J. J. Qin,⁷² L. Q. Qin,¹⁴
 X. S. Qin,⁵⁰ Z. H. Qin,^{1,58} J. F. Qiu,¹ S. Q. Qu,⁶¹ C. F. Redmer,³⁵ K. J. Ren,³⁹ A. Rivetti,^{74c} M. Rolo,^{74c} G. Rong,^{1,63}
 Ch. Rosner,¹⁸ S. N. Ruan,⁴³ N. Salone,⁴⁴ A. Sarantsev,^{36,c} Y. Schelhaas,³⁵ K. Schoenning,⁷⁵ M. Scodeggio,^{29a,29b}
 K. Y. Shan,^{12,f} W. Shan,²⁴ X. Y. Shan,^{71,58} J. F. Shangguan,⁵⁵ L. G. Shao,^{1,63} M. Shao,^{71,58} C. P. Shen,^{12,f} H. F. Shen,^{1,63}
 W. H. Shen,⁶³ X. Y. Shen,^{1,63} B. A. Shi,⁶³ H. C. Shi,^{71,58} J. L. Shi,¹² J. Y. Shi,¹ Q. Q. Shi,⁵⁵ R. S. Shi,^{1,63} X. Shi,^{1,58}
 J. J. Song,¹⁹ T. Z. Song,⁵⁹ W. M. Song,^{34,1} Y. J. Song,¹² Y. X. Song,^{46,g} S. Sosio,^{74a,74c} S. Spataro,^{74a,74c} F. Stieler,³⁵ Y. J. Su,⁶³
 G. B. Sun,⁷⁶ G. X. Sun,¹ H. Sun,⁶³ H. K. Sun,¹ J. F. Sun,¹⁹ K. Sun,⁶¹ L. Sun,⁷⁶ S. S. Sun,^{1,63} T. Sun,^{51,e} W. Y. Sun,³⁴ Y. Sun,⁹
 Y. J. Sun,^{71,58} Y. Z. Sun,¹ Z. T. Sun,⁵⁰ Y. X. Tan,^{71,58} C. J. Tang,⁵⁴ G. Y. Tang,¹ J. Tang,⁵⁹ Y. A. Tang,⁷⁶ L. Y. Tao,⁷²
 Q. T. Tao,^{25,h} M. Tat,⁶⁹ J. X. Teng,^{71,58} V. Thoren,⁷⁵ W. H. Tian,⁵² W. H. Tian,⁵⁹ Y. Tian,^{31,63} Z. F. Tian,⁷⁶ I. Uman,^{62b}
 Y. Wan,⁵⁵ S. J. Wang,⁵⁰ B. Wang,¹ B. L. Wang,⁶³ Bo Wang,^{71,58} C. W. Wang,⁴² D. Y. Wang,^{46,g} F. Wang,⁷² H. J. Wang,^{38,j,k}
 J. P. Wang,⁵⁰ K. Wang,^{1,58} L. L. Wang,¹ M. Wang,⁵⁰ Meng Wang,^{1,63} N. Y. Wang,⁶³ S. Wang,^{12,f} S. Wang,^{38,j,k} T. Wang,^{12,f}
 T. J. Wang,⁴³ W. Wang,⁵⁹ W. Wang,⁷² W. P. Wang,^{71,58} X. Wang,^{46,g} X. F. Wang,^{38,j,k} X. J. Wang,³⁹ X. L. Wang,^{12,f}
 Y. Wang,⁶¹ Y. D. Wang,⁴⁵ Y. F. Wang,^{1,58,63} Y. L. Wang,¹⁹ Y. N. Wang,⁴⁵ Y. Q. Wang,¹ Yaqian Wang,^{17,1} Yi Wang,⁶¹
 Z. Wang,^{1,58} Z. L. Wang,⁷² Z. Y. Wang,^{1,63} Ziyi Wang,⁶³ D. Wei,⁷⁰ D. H. Wei,¹⁴ F. Weidner,⁶⁸ S. P. Wen,¹ C. W. Wenzel,³
 U. Wiedner,³ G. Wilkinson,⁶⁹ M. Wolke,⁷⁵ L. Wollenberg,³ C. Wu,³⁹ J. F. Wu,^{1,8} L. H. Wu,¹ L. J. Wu,^{1,63} X. Wu,^{12,f}
 X. H. Wu,³⁴ Y. Wu,⁷¹ Y. H. Wu,⁵⁵ Y. J. Wu,³¹ Z. Wu,^{1,58} L. Xia,^{71,58} X. M. Xian,³⁹ T. Xiang,^{46,g} D. Xiao,^{38,j,k} G. Y. Xiao,⁴²
 S. Y. Xiao,¹ Y. L. Xiao,^{12,f} Z. J. Xiao,⁴¹ C. Xie,⁴² X. H. Xie,^{46,g} Y. Xie,⁵⁰ Y. G. Xie,^{1,58} Y. H. Xie,⁶ Z. P. Xie,^{71,58}

T. Y. Xing,^{1,63} C. F. Xu,^{1,63} C. J. Xu,⁵⁹ G. F. Xu,¹ H. Y. Xu,⁶⁶ Q. J. Xu,¹⁶ Q. N. Xu,³⁰ W. Xu,¹ W. L. Xu,⁶⁶ X. P. Xu,⁵⁵ Y. C. Xu,⁷⁸ Z. P. Xu,⁴² Z. S. Xu,⁶³ F. Yan,^{12,f} L. Yan,^{12,f} W. B. Yan,^{71,58} W. C. Yan,⁸¹ X. Q. Yan,¹ H. J. Yang,^{51,e} H. L. Yang,³⁴ H. X. Yang,¹ Tao Yang,¹ Y. Yang,^{12,f} Y. F. Yang,⁴³ Y. X. Yang,^{1,63} Yifan Yang,^{1,63} Z. W. Yang,^{38,j,k} Z. P. Yao,⁵⁰ M. Ye,^{1,58} M. H. Ye,⁸ J. H. Yin,¹ Z. Y. You,⁵⁹ B. X. Yu,^{1,58,63} C. X. Yu,⁴³ G. Yu,^{1,63} J. S. Yu,^{25,h} T. Yu,⁷² X. D. Yu,^{46,g} C. Z. Yuan,^{1,63} L. Yuan,² S. C. Yuan,¹ Y. Yuan,^{1,63} Z. Y. Yuan,⁵⁹ C. X. Yue,³⁹ A. A. Zafar,⁷³ F. R. Zeng,⁵⁰ S. H. Zeng,⁷² X. Zeng,^{12,f} Y. Zeng,^{25,h} Y. J. Zeng,^{1,63} X. Y. Zhai,³⁴ Y. C. Zhai,⁵⁰ Y. H. Zhan,⁵⁹ A. Q. Zhang,^{1,63} B. L. Zhang,^{1,63} B. X. Zhang,¹ D. H. Zhang,⁴³ G. Y. Zhang,¹⁹ H. Zhang,⁷¹ H. C. Zhang,^{1,58,63} H. H. Zhang,⁵⁹ H. H. Zhang,³⁴ H. Q. Zhang,^{1,58,63} H. Y. Zhang,^{1,58} J. Zhang,⁵⁹ J. Zhang,⁸¹ J. J. Zhang,⁵² J. L. Zhang,²⁰ J. Q. Zhang,⁴¹ J. W. Zhang,^{1,58,63} J. X. Zhang,^{38,j,k} J. Y. Zhang,¹ J. Z. Zhang,^{1,63} Jianyu Zhang,⁶³ L. M. Zhang,⁶¹ L. Q. Zhang,⁵⁹ Lei Zhang,⁴² P. Zhang,^{1,63} Q. Y. Zhang,^{39,81} Shuihan Zhang,^{1,63} Shulei Zhang,^{25,h} X. D. Zhang,⁴⁵ X. M. Zhang,¹ X. Y. Zhang,⁵⁰ Y. Zhang,⁷² Y. Zhang,⁶⁹ Y. T. Zhang,⁸¹ Y. H. Zhang,^{1,58} Yan Zhang,^{71,58} Yao Zhang,¹ Z. D. Zhang,¹ Z. H. Zhang,¹ Z. L. Zhang,³⁴ Z. Y. Zhang,⁴³ Z. Y. Zhang,⁷⁶ G. Zhao,¹ J. Y. Zhao,^{1,63} J. Z. Zhao,^{1,58} Lei Zhao,^{71,58} Ling Zhao,¹ M. G. Zhao,⁴³ R. P. Zhao,⁶³ S. J. Zhao,⁸¹ Y. B. Zhao,^{1,58} Y. X. Zhao,^{31,63} Z. G. Zhao,^{71,58} A. Zhemchugov,^{36,a} B. Zheng,⁷² J. P. Zheng,^{1,58} W. J. Zheng,^{1,63} Y. H. Zheng,⁶³ B. Zhong,⁴¹ X. Zhong,⁵⁹ H. Zhou,⁵⁰ L. P. Zhou,^{1,63} X. Zhou,⁷⁶ X. K. Zhou,⁶ X. R. Zhou,^{71,58} X. Y. Zhou,³⁹ Y. Z. Zhou,^{12,f} J. Zhu,⁴³ K. Zhu,¹ K. J. Zhu,^{1,58,63} L. Zhu,³⁴ L. X. Zhu,⁶³ S. H. Zhu,⁷⁰ S. Q. Zhu,⁴² T. J. Zhu,^{12,f} W. J. Zhu,^{12,f} Y. C. Zhu,^{71,58} Z. A. Zhu,^{1,63} J. H. Zou,¹ and J. Zu^{71,58}

(BESIII Collaboration)

- ¹*Institute of High Energy Physics, Beijing 100049, People's Republic of China*
²*Beihang University, Beijing 100191, People's Republic of China*
³*Bochum Ruhr-University, D-44780 Bochum, Germany*
⁴*Budker Institute of Nuclear Physics SB RAS (BINP), Novosibirsk 630090, Russia*
⁵*Carnegie Mellon University, Pittsburgh, Pennsylvania 15213, USA*
⁶*Central China Normal University, Wuhan 430079, People's Republic of China*
⁷*Central South University, Changsha 410083, People's Republic of China*
⁸*China Center of Advanced Science and Technology, Beijing 100190, People's Republic of China*
⁹*China University of Geosciences, Wuhan 430074, People's Republic of China*
¹⁰*Chung-Ang University, Seoul, 06974, Republic of Korea*
¹¹*COMSATS University Islamabad, Lahore Campus, Defence Road, Off Raiwind Road, 54000 Lahore, Pakistan*
¹²*Fudan University, Shanghai 200433, People's Republic of China*
¹³*GSI Helmholtzcentre for Heavy Ion Research GmbH, D-64291 Darmstadt, Germany*
¹⁴*Guangxi Normal University, Guilin 541004, People's Republic of China*
¹⁵*Guangxi University, Nanning 530004, People's Republic of China*
¹⁶*Hangzhou Normal University, Hangzhou 310036, People's Republic of China*
¹⁷*Hebei University, Baoding 071002, People's Republic of China*
¹⁸*Helmholtz Institute Mainz, Staudinger Weg 18, D-55099 Mainz, Germany*
¹⁹*Henan Normal University, Xinxiang 453007, People's Republic of China*
²⁰*Henan University, Kaifeng 475004, People's Republic of China*
²¹*Henan University of Science and Technology, Luoyang 471003, People's Republic of China*
²²*Henan University of Technology, Zhengzhou 450001, People's Republic of China*
²³*Huangshan College, Huangshan 245000, People's Republic of China*
²⁴*Hunan Normal University, Changsha 410081, People's Republic of China*
²⁵*Hunan University, Changsha 410082, People's Republic of China*
²⁶*Indian Institute of Technology Madras, Chennai 600036, India*
²⁷*Indiana University, Bloomington, Indiana 47405, USA*
^{28a}*INFN Laboratori Nazionali di Frascati, INFN Laboratori Nazionali di Frascati, I-00044 Frascati, Italy*
^{28b}*INFN Sezione di Perugia, I-06100 Perugia, Italy*
^{28c}*University of Perugia, I-06100 Perugia, Italy*
^{29a}*INFN Sezione di Ferrara, INFN Sezione di Ferrara, I-44122 Ferrara, Italy*
^{29b}*University of Ferrara, I-44122 Ferrara, Italy*
³⁰*Inner Mongolia University, Hohhot 010021, People's Republic of China*
³¹*Institute of Modern Physics, Lanzhou 730000, People's Republic of China*
³²*Institute of Physics and Technology, Peace Avenue 54B, Ulaanbaatar 13330, Mongolia*
³³*Instituto de Alta Investigación, Universidad de Tarapacá, Casilla 7D, Arica 1000000, Chile*

- ³⁴*Jilin University, Changchun 130012, People's Republic of China*
- ³⁵*Johannes Gutenberg University of Mainz, Johann-Joachim-Becher-Weg 45, D-55099 Mainz, Germany*
- ³⁶*Joint Institute for Nuclear Research, 141980 Dubna, Moscow region, Russia*
- ³⁷*Justus-Liebig-Universität Giessen, II. Physikalisches Institut, Heinrich-Buff-Ring 16, D-35392 Giessen, Germany*
- ³⁸*Lanzhou University, Lanzhou 730000, People's Republic of China*
- ³⁹*Liaoning Normal University, Dalian 116029, People's Republic of China*
- ⁴⁰*Liaoning University, Shenyang 110036, People's Republic of China*
- ⁴¹*Nanjing Normal University, Nanjing 210023, People's Republic of China*
- ⁴²*Nanjing University, Nanjing 210093, People's Republic of China*
- ⁴³*Nankai University, Tianjin 300071, People's Republic of China*
- ⁴⁴*National Centre for Nuclear Research, Warsaw 02-093, Poland*
- ⁴⁵*North China Electric Power University, Beijing 102206, People's Republic of China*
- ⁴⁶*Peking University, Beijing 100871, People's Republic of China*
- ⁴⁷*Qufu Normal University, Qufu 273165, People's Republic of China*
- ⁴⁸*Renmin University of China, Beijing 100872, People's Republic of China*
- ⁴⁹*Shandong Normal University, Jinan 250014, People's Republic of China*
- ⁵⁰*Shandong University, Jinan 250100, People's Republic of China*
- ⁵¹*Shanghai Jiao Tong University, Shanghai 200240, People's Republic of China*
- ⁵²*Shanxi Normal University, Linfen 041004, People's Republic of China*
- ⁵³*Shanxi University, Taiyuan 030006, People's Republic of China*
- ⁵⁴*Sichuan University, Chengdu 610064, People's Republic of China*
- ⁵⁵*Soochow University, Suzhou 215006, People's Republic of China*
- ⁵⁶*South China Normal University, Guangzhou 510006, People's Republic of China*
- ⁵⁷*Southeast University, Nanjing 211100, People's Republic of China*
- ⁵⁸*State Key Laboratory of Particle Detection and Electronics, Beijing 100049, Hefei 230026, People's Republic of China*
- ⁵⁹*Sun Yat-Sen University, Guangzhou 510275, People's Republic of China*
- ⁶⁰*Suranaree University of Technology, University Avenue 111, Nakhon Ratchasima 30000, Thailand*
- ⁶¹*Tsinghua University, Beijing 100084, People's Republic of China*
- ^{62a}*Turkish Accelerator Center Particle Factory Group, Istinye University, 34010 Istanbul, Turkey*
- ^{62b}*Near East University, Nicosia, North Cyprus, 99138, Mersin 10, Turkey*
- ⁶³*University of Chinese Academy of Sciences, Beijing 100049, People's Republic of China*
- ⁶⁴*University of Groningen, NL-9747 AA Groningen, The Netherlands*
- ⁶⁵*University of Hawaii, Honolulu, Hawaii 96822, USA*
- ⁶⁶*University of Jinan, Jinan 250022, People's Republic of China*
- ⁶⁷*University of Manchester, Oxford Road, Manchester, M13 9PL, United Kingdom*
- ⁶⁸*University of Muenster, Wilhelm-Klemm-Strasse 9, 48149 Muenster, Germany*
- ⁶⁹*University of Oxford, Keble Road, Oxford OX13RH, United Kingdom*
- ⁷⁰*University of Science and Technology Liaoning, Anshan 114051, People's Republic of China*
- ⁷¹*University of Science and Technology of China, Hefei 230026, People's Republic of China*
- ⁷²*University of South China, Hengyang 421001, People's Republic of China*
- ⁷³*University of the Punjab, Lahore-54590, Pakistan*
- ^{74a}*University of Turin and INFN, University of Turin, I-10125 Turin, Italy*
- ^{74b}*University of Eastern Piedmont, I-15121 Alessandria, Italy*
- ^{74c}*INFN, I-10125, Turin, Italy*
- ⁷⁵*Uppsala University, Box 516, SE-75120 Uppsala, Sweden*
- ⁷⁶*Wuhan University, Wuhan 430072, People's Republic of China*
- ⁷⁷*Xinyang Normal University, Xinyang 464000, People's Republic of China*
- ⁷⁸*Yantai University, Yantai 264005, People's Republic of China*
- ⁷⁹*Yunnan University, Kunming 650500, People's Republic of China*
- ⁸⁰*Zhejiang University, Hangzhou 310027, People's Republic of China*
- ⁸¹*Zhengzhou University, Zhengzhou 450001, People's Republic of China*

^aAlso at the Moscow Institute of Physics and Technology, Moscow 141700, Russia.

^bAlso at the Novosibirsk State University, Novosibirsk 630090, Russia.

^cAlso at the NRC "Kurchatov Institute," PNPI, 188300 Gatchina, Russia.

^dAlso at Goethe University Frankfurt, 60323 Frankfurt am Main, Germany.

^eAlso at Key Laboratory for Particle Physics, Astrophysics and Cosmology, Ministry of Education; Shanghai Key Laboratory for Particle Physics and Cosmology; Institute of Nuclear and Particle Physics, Shanghai 200240, People's Republic of China.

^fAlso at Key Laboratory of Nuclear Physics and Ion-beam Application (MOE) and Institute of Modern Physics, Fudan University, Shanghai 200443, People's Republic of China.

^gAlso at State Key Laboratory of Nuclear Physics and Technology, Peking University, Beijing 100871, People's Republic of China.

^hAlso at School of Physics and Electronics, Hunan University, Changsha 410082, China.

ⁱAlso at Guangdong Provincial Key Laboratory of Nuclear Science, Institute of Quantum Matter, South China Normal University, Guangzhou 510006, China.

^jAlso at MOE Frontiers Science Center for Rare Isotopes, Lanzhou University, Lanzhou 730000, People's Republic of China.

^kAlso at Lanzhou Center for Theoretical Physics, Lanzhou University, Lanzhou 730000, People's Republic of China.

^lAlso at the Department of Mathematical Sciences, IBA, Karachi 75270, Pakistan.